Effect of Solvent on the Properties of Thermoplastic Polyurethane/Clay Nanocomposites Prepared by Solution Mixing

Cheol Ho Dan, Young Doo Kim, Minho Lee, Byong Hun Min, Jeong Ho Kim

Department of Chemical Engineering, University of Suwon, Kyunggido, Korea

Received 23 March 2007; accepted 26 November 2007
DOI 10.1002/app.27879
Published online 4 February 2008 in Wiley InterScience (www.interscience.wiley.com).

ABSTRACT: Effect of different solvents on the clay dispersion and the final properties of the thermoplastic polyurethanes (TPUs)/clay nanocomposites prepared via solution mixing was studied. The polyether- and polyester-based TPUs were used along with organically modified clays (C30B, C25A, and C15A) and the pristine montmorillonite (PM). Dimethylacetamide (DMAc) and tetrahydrofuran (THF) were used as solvents for solution mixing. Nanocomposites containing C30B prepared from DMAc solution showed the better clay dispersion than the ones from THF solution, while THF gave the better dispersion of clays for nanocomposites containing C15A. Morphologies of the nanocomposites were observed to be determined not only by the state of clay dispersion in different solvents but also by the interaction between the polymer and the specific clay. Affinity between solvents and clays becomes important when there is no specific interaction between the clay and the polymer of interest, or when the interaction between the two is rather weak. The compatibility between clays and polymers becomes dominating if there exists a specific interaction between the two. FTIR analysis was conducted to study the interactions involved in the nanocomposites. Dynamic mechanical properties measurement was also carried out to see the effect of solvents. © 2008 Wiley Periodicals, Inc. J Appl Polym Sci 108: 2128–2138, 2008

Key words: polyurethane; nanocomposites; morphology

INTRODUCTION

Since the research on nylon 6/montmorillonite was reported by Toyota, a number of studies on polymer/clay nanocomposites have been carried out showing the remarkable improvement in various properties as compared with those of conventional composites.[1–16] Dispersion of clays in polymer nanocomposites usually depends on the preparation method of nanocomposites, and the interaction between polymer matrix and organoclay.[17–20] In this study, solution mixing method was used for the preparation of nanocomposites where the nature of solvents is critical in determining the clay dispersion in the nanocomposites.

Thermoplastic polyurethanes (TPUs) are usually formed from polyether or polyester polyols and aliphatic or aromatic diisocyanates.[21–26] Since the first study on polyurethane/clay nanocomposites by Wang and Pinnavaia,[27] many studies have been carried out. Tien and Wei reported the completely exfoliated PU/clay nanocomposites by *in situ* polymerization using 12-amino lauric acid and benzidine.[28,29] Pattanayak and Jana reported that the exfoliated nanocomposites of TPUs can be prepared by some unique preparation method resulting in remarkable increase in tensile strength and modulus along with optical clarity when compared with pure polyurethanes.[30–32] In our previous research, nanocomposites of TPUs with various clays were prepared by melt-mixing to study the effect of different clay modifiers on the morphology and physical properties of TPU nanocomposites.[33]

In this study, nanocomposites of TPU and clays with varying degree of hydrophobicity such as PM, C30B, C25A, and C15A were prepared by solution mixing to study the effect of solvents having different degree of polarity on the dispersion of clays in the nanocomposites. Also, the morphology and mechanical properties of polyurethane/clay nanocomposites were investigated along with the analysis using FTIR. The difference with our previous study on TPU/clay nanocomposites prepared by melt-mixing[33] is that decomposition of organic modifiers in the clay which can occur during melt mixing can be avoided in nanocomposites prepared by solution mixing in the present study since solution mixing is carried out around the room temperature.

EXPERIMENTAL

Materials and methods

Two types of TPUs were obtained from SK Chemicals (Suwon, Korea), polyether-based TPU (Skythane

Correspondence to: J. H. Kim (jhkim@suwon.ac.kr).

Journal of Applied Polymer Science, Vol. 108, 2128–2138 (2008)

R185A, M_w = 250,000) and polyester-based TPU (Skythane S185A, M_w = 250,000) having the similar Shore Hardness of 87A. Hard segments of both ether-type and ester-type TPUs are made of 4,4′-diphenylmethane diisocyanate (MDI) and 1,4-butanediol (BD), but soft segments are different such as poly(tetramethylene oxide) glycol (PTMG, M_w = 1000) for ether type and poly(butylene adipate) glycol (PBAG, M_w = 1000) for ester type.

Three types of organically modified clays and natural clays were obtained from Southern Clay Products (Gonzales, TX). Pristine montmorillonite, Cloisite Na^+ (PM) has the cation-exchange capacity (CEC) of 92.6 mequiv/100 g clay. Organically modified montmorillonite, Cloisite 25A (C25A, CEC: 95 mequiv/100 g) and Cloisite 15A (C15A, CEC: 125 mequiv/100 g) are montmorillonites modified with dimethyl, hydrogenated tallow, 2-ethylhexyl quaternary ammonium ion, and dimethyl, dehydrogenated tallow quaternary ammonium ion, respectively. Cloisite 30B (C30B, CEC: 90 mequiv/100 g) is a montmorillonite modified with a quaternary ammonium salt having one methyl, one tallow, and two $—CH_2CH_2OH$ groups. PM has the highest hydrophilicity and 15A has the lowest, while clay 25A and C30B are located between the two.

The TPU nanocomposites were prepared as follows: 5 wt % clay solution was sonicated before being mixed with TPU solution. Two different solvents used in this study were *N,N*-dimethylacetamide (DMAc, Sigma-Aldrich, Korea) and tetrahydrofuran (THF, Sigma-Aldrich, Korea). Solutions of TPUs with clays were stirred for 4 h at room temperature with magnetic stirrer. The mixture was then cast onto glass plate and the resulting film was dried at 50°C for 36 h followed by subsequent drying for 48 h under vacuum at the same temperature.

Characterization

The change in gallery distance of silicate layers in the clay was determined on X-ray diffractometer (D-8 Advance) using Cu Kα radiation at 40 kV, 35 mA. The samples were scanned at 2°/min. The basal spacing of the clay, d_{001} was calculated using the Bragg's law ($\lambda = 2d\sin\theta$).

TEM images of nanocomposite specimens were obtained using energy filtering-transmission electron microscopy (EM-912 OMEGA, Carl Zeiss, Germany) with operating voltage of 120 kV at the Korea Basic Science Institute. The ultra-thin sectioning was performed on ultra-microtome at −100°C.

Fourier transform infrared spectroscopy (FTIR) was performed on FTIR-4200 (Jasco, Japan) at a resolution of 4 cm^{-1}. Dynamic mechanical tests were performed using a dynamic mechanical analyzer (TA Instruments DMA 2980, New Castle, DE) with amplitude of 0.2% at a frequency of 2 Hz. The temperature was increased at a heating rate of 2°C/min over the temperature range from −100 to 100°C.

RESULTS AND DISCUSSION

Morphology

Figures 1–4 show X-ray diffraction (XRD) patterns for nanocomposites of both polyether-based TPUs (ether-TPU) and polyester based TPUs (ester-TPU) with various clays prepared from DMAc or THF solutions with 5 wt % clay loadings. XRD results for ether- and ester-TPUs with PM prepared using DMAc and THF are shown in Figure 1(a,b), respectively. In these two figures, peaks from clay PM are observed in both ether- and ester-TPU/PM, regard-

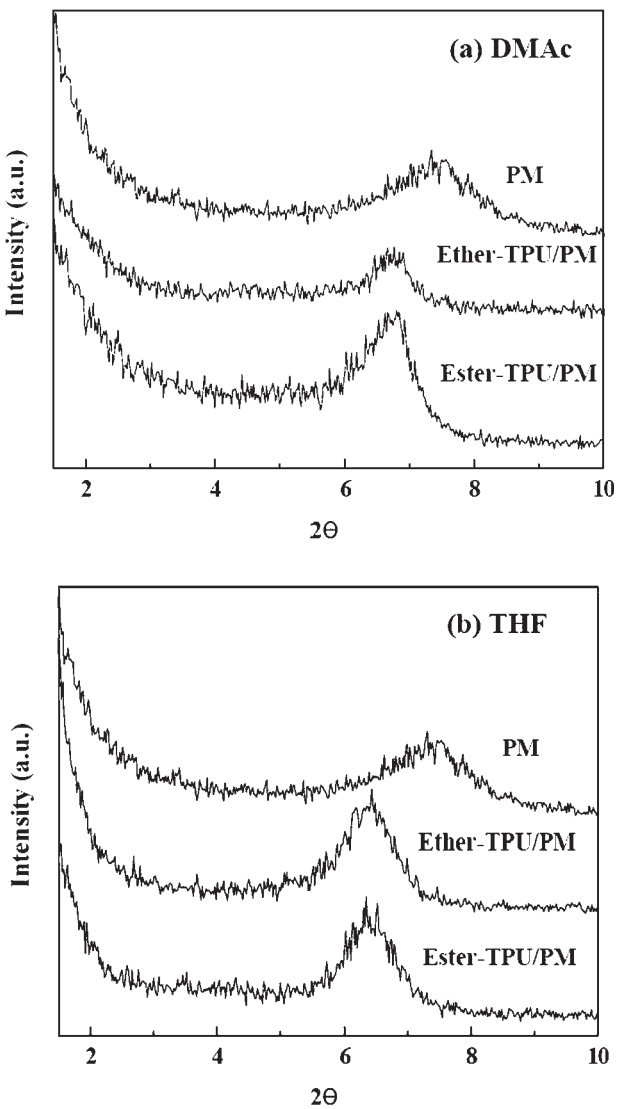

Figure 1 XRD patterns of ether- and ester-TPU nanocomposites with 5 wt % of PM prepared in (a) DMAc and (b) THF.

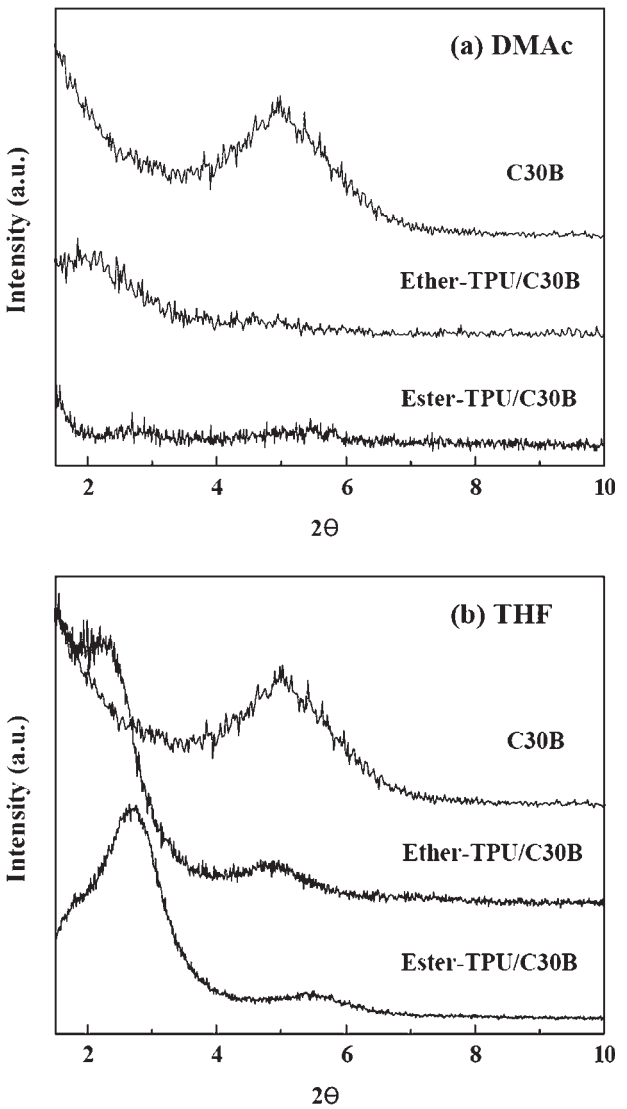

Figure 2 XRD patterns of ether- and ester-TPU nanocomposites with 5 wt % of C30B prepared in (a) DMAc and (b) THF.

less of the kind of solvent used, although there is a little decrease in 2θ values. This means that clay PM is not well dispersed in both TPUs. Figure 2(a) shows the XRD results for the nanocomposites containing C30B prepared using DMAc. The peak of clay C30B itself is observed at 2θ = 4.8° (*d*-spacing of 1.85 nm), while almost no peaks are shown in ether- and ester-TPU/C30B. This result indicates that very good dispersion close to exfoliation was formed in both nanocomposites prepared from DMAc solution. The good dispersion of the silicate layers of C30B may be attributed to the specific interaction originated from hydrogen bonding between carbonyl groups in TPU and hydroxyl groups in C30B as reported in the previous study.[33] The XRD results prepared from THF are shown in Figure 2(b). Although these results exhibit two peaks at 2θ = 2.3° (d_{001}-spacing = 3.86 nm) and 4.7° (d_{002}-spacing = 1.89 nm) for ether-TPU/C30B and peaks at 2θ = 2.7° (d_{001}-spacing = 3.27 nm) and 5.5° (d_{002}-spacing = 1.61 nm) for ester-TPU/C30B, the interlayer spacing of C30B also appears to increase in both cases. The presence of peaks indicates that clay dispersion of nanocomposites from THF is not so good as that obtained from DMAc solution.

The XRD patterns of C25A and TPU/C25A nanocomposites prepared from DMAc are shown in Figure 3(a). A peak of clay C25A appears at 2θ = 4.5° (*d*-spacing = 1.96 nm), while ether- and ester-TPU/C25A nanocomposites show peaks at 2θ = 3.1° (*d*-spacing = 2.94 nm) and 2θ = 3.3° (*d*-spacing = 2.68 nm), respectively. These results indicate that the *d*-spacing of C25A showed a small increase in TPU/C25A. Ether- and ester-TPU/C25A nanocomposites prepared from THF solution as in Figure 3(b) showed

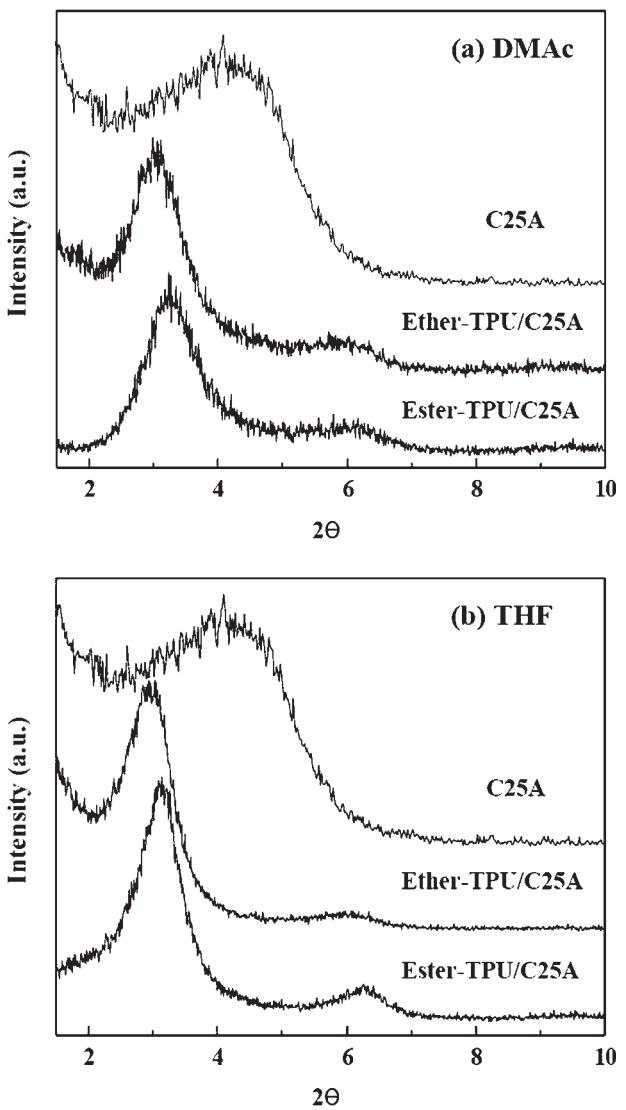

Figure 3 XRD patterns of ether- and ester-TPU nanocomposites with 5 wt % of C25A prepared in (a) DMAc and (b) THF.

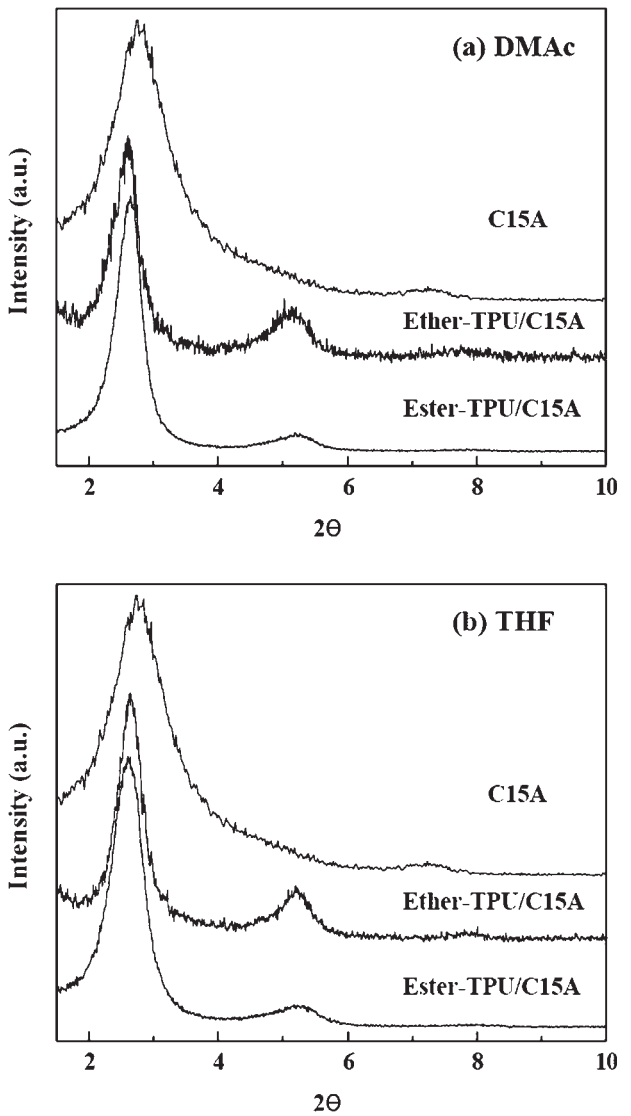

Figure 4 XRD patterns of ether- and ester-TPU nanocomposites with 5 wt % of C15A prepared in (a) DMAc and (b) THF.

that the two peak positions are same as those of TPU/C25A prepared from DMAc solution, implying that the clay C25A behaves in a similar manner in both solvents. Figure 4(a) shows XRD patterns of C15A, ether- and ester-TPU/C15A prepared from DMAc solution. A quite small increase in the d_{001}-spacing in this case from 3.15 nm ($2\theta = 2.8^\circ$) of C15A to 3.4 nm ($2\theta = 2.6^\circ$) of both ether- and ester-TPU nanocomposites suggests that just a small portion of polyurethane chain is intercalated into clay layers. The increase in d_{002}-spacing of ester and ether-TPU/C15A nanocomposites (from 1.22 to 1.68 nm) also indicates that nanocomposites have a partially intercalated structure. TPU/C15A nanocomposites prepared from THF exhibit almost similar result as that of the ones prepared from DMAc.

To see the morphologies of TPU nanocomposites, TEM pictures were taken for samples containing C30B or C15A prepared from DMAc or THF as shown in Figure 5 through 8. The TEM image of ether-TPU/C30B prepared from DMAc solution is shown in Figure 5(a). In the 500-nm scale TEM image, platelets of clay C30B were observed to show good dispersion close to exfoliation. In the 50-nm scale image, two or three layers of clays were observed. This result is consistent with the previous XRD results where almost no peaks were observed. Figure 5(b) shows the clay dispersion for the ester-TPU/C30B from DMAc. Again a very good dispersion is observed. In the 50-nm scale picture, around four layers were observed for one clay particle.

Figure 6(a,b) shows the TEM images for ether- and ester-TPU/C30B nanocomposites, respectively, prepared from THF solution. In these TEM images, thicker particles are observed when compared with Figure 5(a,b). Still, the clay particles show some degree of dispersion even when they are prepared from THF solution, which is consistent with the XRD result where the clay interlayer *d*-spacing showed some increase as compared with that of pure C30B. Poorer dispersion of clays in nanocomposites from THF when compared with DMAc may be originated, from which not much THF molecules could go into the interlayers of C30B because of the lack of compatibility between THF and clay, while DMAc caused enough swelling of C30B. The solubility parameter of DMAc is 22.7 $MPa^{1/2}$ and that of THF is 19.4 $MPa^{1/2}$. Both solvents have the similar value of dispersion contribution to solubility parameter (δ) but the difference is that DMAc has higher value of polar and hydrogen bonding contribution to δ.

TEM images of Figure 7 show the dispersion of clay C15A in ether-TPU/C15A [Fig. 7(a)] and ester-TPU/C15A nanocomposites [Fig. 7(b)] prepared from DMAc. Thick aggregated clay particles are observed in both cases indicating poor dispersion of clay C15A. TEM images for ether- and ester-TPUs with C15A prepared from THF solution are shown in Figure 8(a,b), respectively, where the clay particles are observed to be much thinner than the ones in Figure 7. This again can be explained by the argument that THF has better affinity to clay C15A than DMAc or in terms of hydrophobicity of solvents and modified clays. From the 50-nm scale, TEM image of Figure 8(a,b), around 7–10 layers are observed for one clay particle showing some degree of intercalation of clay C15A.

All the above results indicate that C30B is more compatible with DMAc than THF, and C15A is more compatible with THF than DMAc. To evaluate the compatibility between clays and solvents by clay dispersion in two solvents, 5 wt % clays PM, C30B,

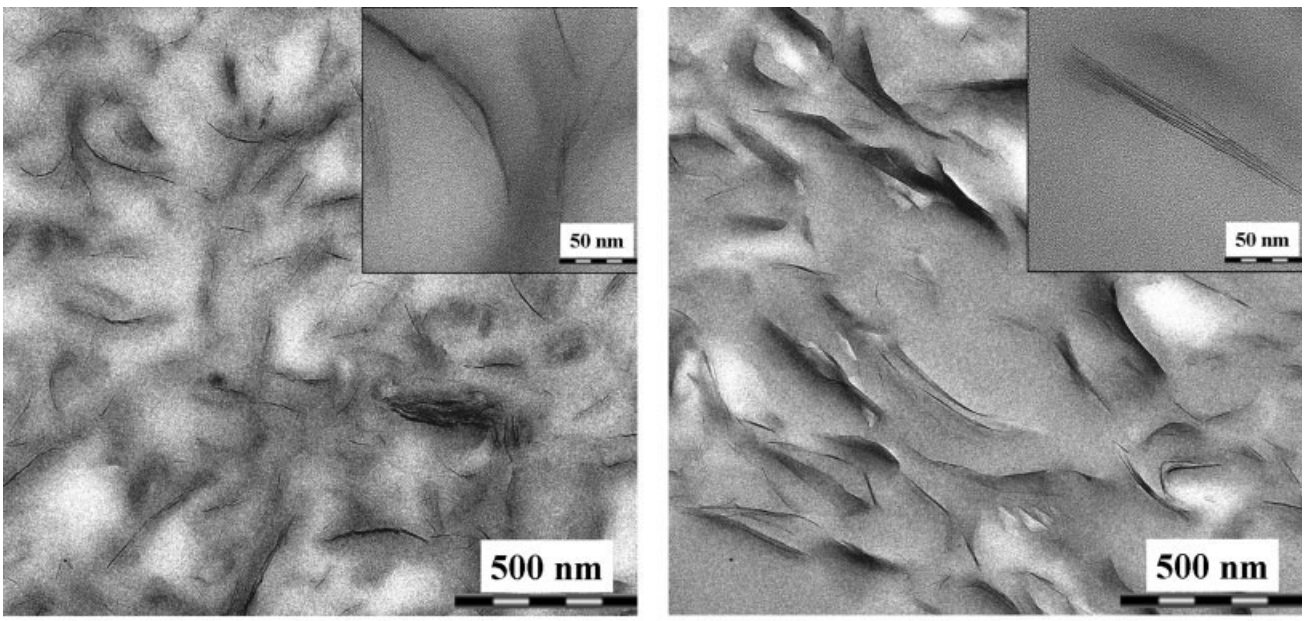

Figure 5 TEM images of (a) ether-TPU nanocomposites and (b) ester-TPU nanocomposites with 5 wt % of C30B prepared in DMAc.

C25A, and C15A were put into DMAc or THF and were mixed for 4 h on magnetic stirrer followed by keeping them for 24 h at room temperature. As shown in Figure 9(a), most clay deposits were observed at the bottom of the vial in case of C15A in DMAc while best dispersion was observed for clay C30B in DMAc. One thing to be noted is that C25A and C15A have about the same modifier, and the only difference between C25A and C15A is that the organic modifier of C15A has longer alkyl chain than that of C25A at one branch of quaternary ammonium ion and also, C15A has a larger modifier

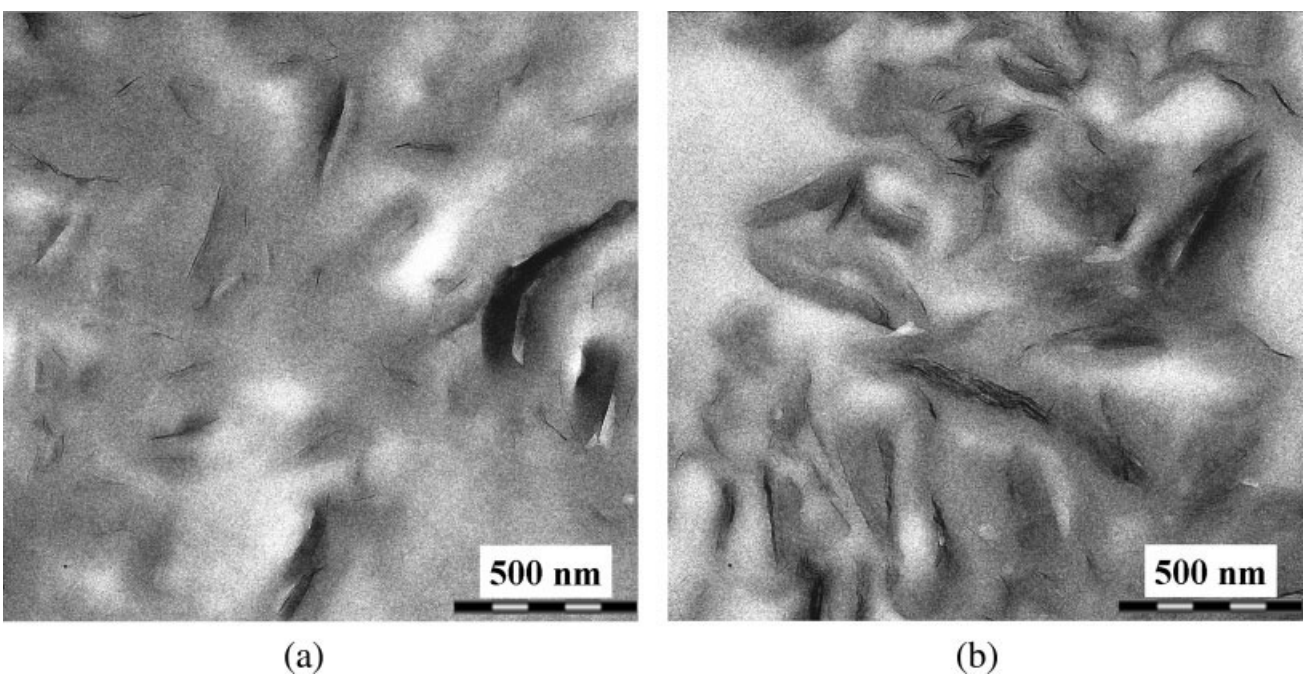

Figure 6 TEM images of (a) ether-TPU nanocomposites and (b) ester-TPU nanocomposites with 5 wt % of C30B prepared in THF.

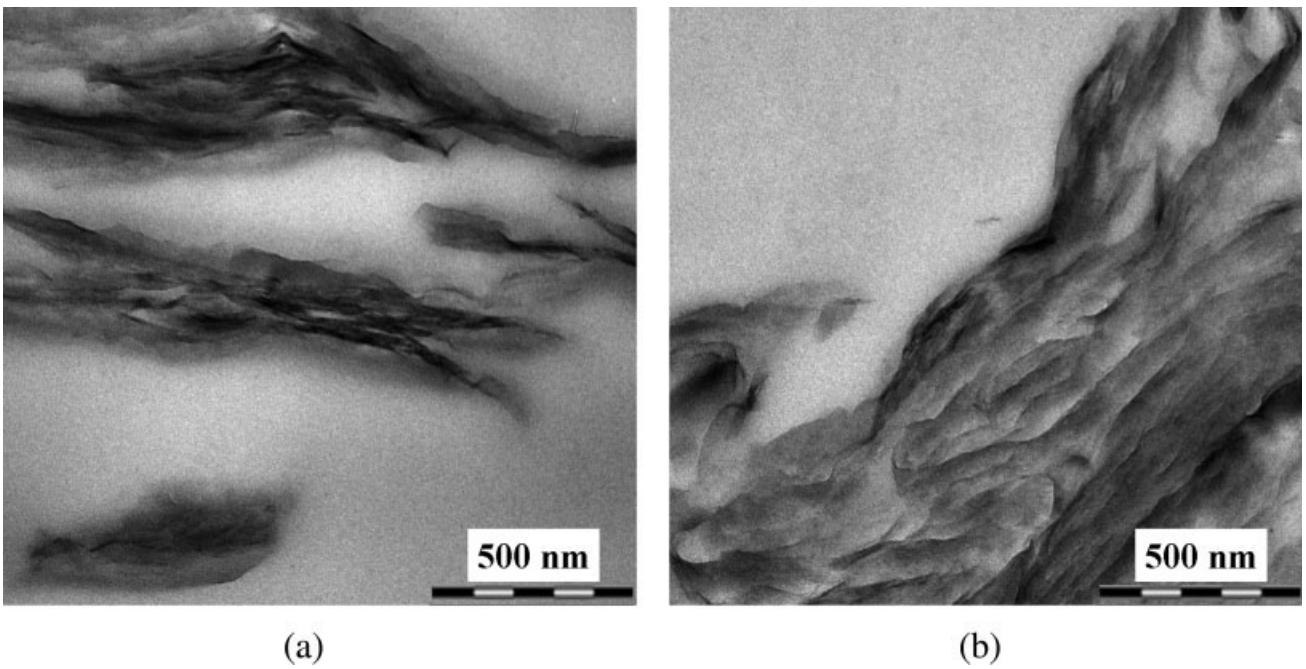

Figure 7 TEM images of (a) ether-TPU nanocomposites and (b) ester-TPU nanocomposites with 5 wt % of C15A prepared in DMAc.

concentration than C25A. Although, there is a report in the literature that the modifiers existing in excess of the ion exchange capacity of natural clay (PM) reside primarily in the interlayer, not on the outer surface of clay,[34] the possibility that some of the excess modifier can still exist outside the surface of the clay cannot be excluded completely. Clay 15A may be regarded as almost hydrophobic in nature from the result of the above experiment on clay dispersion in DMAc, since almost complete segregation of C15A clays at the bottom of the vial was observed. In this regard, very little inorganic clay surface seems to be exposed to solvent and most of the C15A clay surface may be thought to be covered by aliphatic

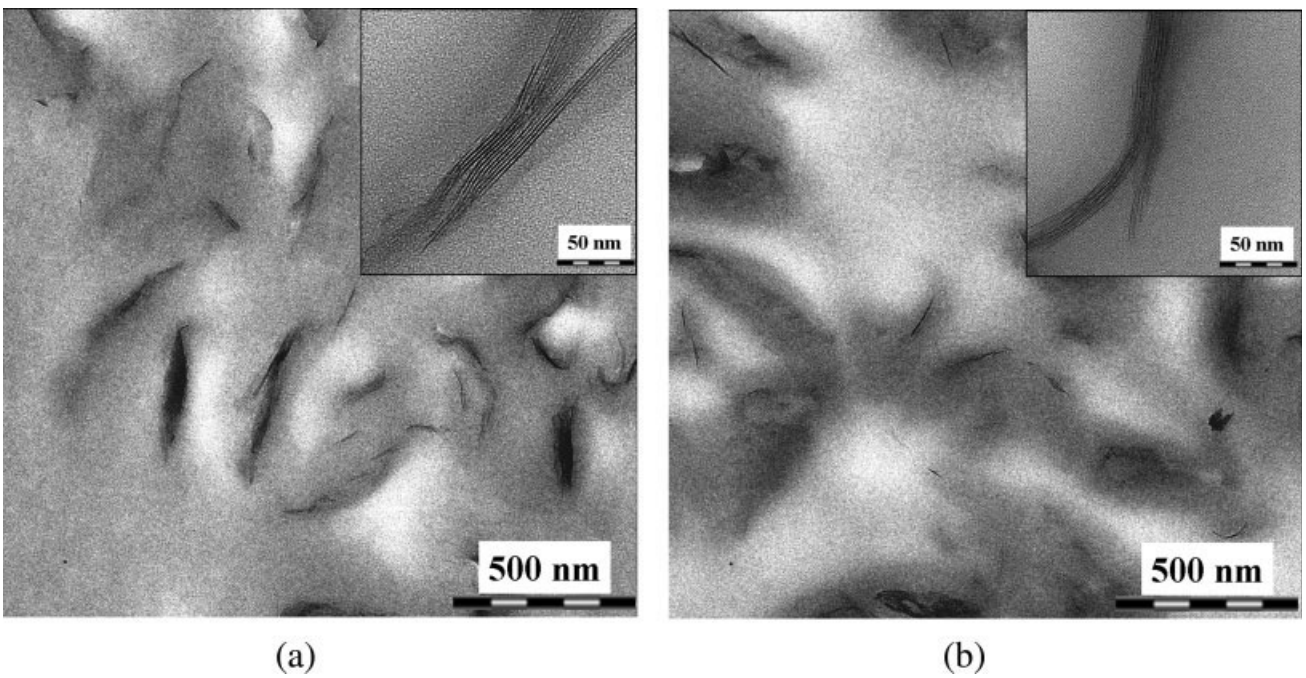

Figure 8 TEM images of (a) ether-TPU nanocomposites and (b) ester-TPU nanocomposites with 5 wt % of C15A prepared in THF.

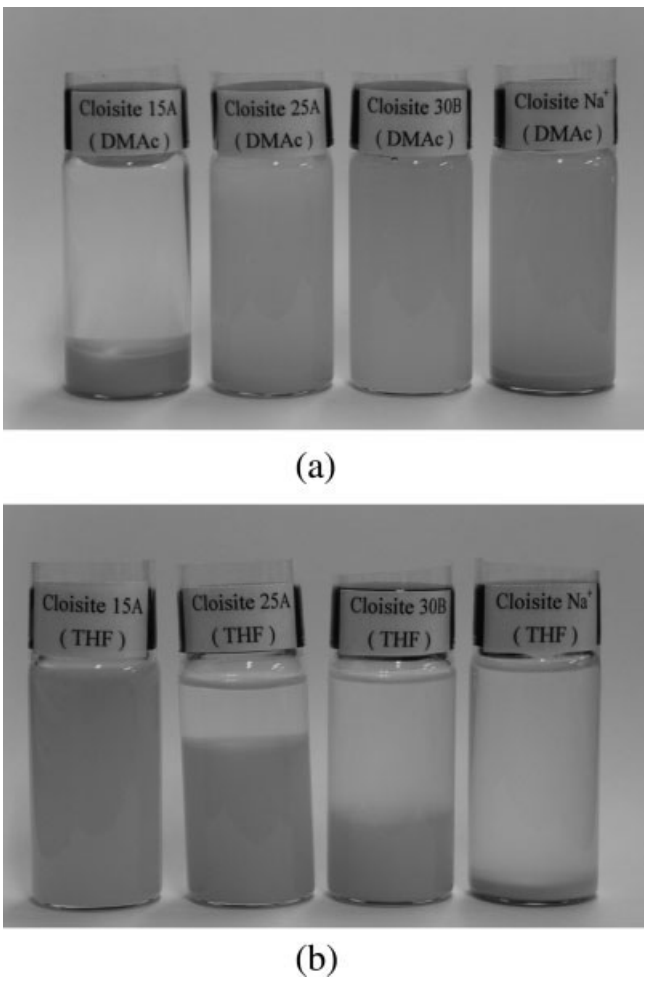

Figure 9 Suspension state of PM, C30B, C25A, and C15A in (a) DMAc and (b) THF.

modifiers. Clay C25A does not possess excess modifiers as C15A does. This may leave some surface of the hydrophilic clay exposed to solvents which is actually thought to be the case, since C25A is observed to be fairly well-dispersed in DMAc while C15A with the similar modifier is not. The balance of this hydrophilic surface and the hydrophobic modifier makes 25A more similar to the nature of ester- or ether-TPUs, which may explain the increase in the interlayer spacing of C25A observed in XRD analysis.

In case of clays in THF shown in Figure 9(b), on the contrary to the DMAc case, only C15A does not show any deposits of clay at the bottom of the vial, while clays PM, C30B, and C25A in THF show two separated phases, which are pure solvent phase and clay dispersed phase in the vials. The height of clay-containing phase shows minimum for clay PM followed by C30B and C25A, where the hydrophobicity of clay increases in the same order.

This observation suggests that PM, C30B, and C25A can be better effectively dispersed in TPU matrix in DMAc while C15A can be in THF. But in the XRD and TEM results, best dispersion of clay in TPU matrix is obtained in nanocomposites containing C30B regardless of the solvent. This indicates that predispersion of clay in the solvent is not a sufficient condition for clay dispersion in TPU nanocomposites. Interaction between the specific clay and the TPU is observed to be a more important factor for the final dispersion of clay in the nanocomposites, although the predispersion of clay in the solvent can do some role and also facilitate the dispersion of clay in the nanocomposites when the interaction between clays and the polymer is not noticeably strong.

Comparison with nanocomposites prepared by melt-mixing

If nanocomposites are prepared by melt-mixing in the extruder, shear from the extrusion may make the layer separation easier, since the modifiers inside the layer weakens the electrostatic force between silicate layers as compared with PM. But in the case of solvent mixing, shear force is much smaller than melt-mixing and the affinity between clays and polymers becomes much more important and becomes the dominating factor for clay dispersion, although there can be a so-called solvent effect in the polymer-clay-solvent ternary system, which is usually not the case.

The clay dispersions of TPU/C30B and TPU/C15A prepared by melt-mixing shown in TEM images of our previous study[33] look very similar to those of TPU/C30B prepared from DMAc and TPU/C15A from THF in this study, respectively. This indicates that good predispersion of clays during solution mixing is important to get good clay dispersion in the final nanocomposites, and also the clay dispersion in nanocomposites prepared by melt-mixing is as good as that obtained by solution mixing. Regarding XRD analyses, similar XRD results were observed for melt-mixed nanocomposites, and solution mixed ones where TPU nanocomposites containing C30B and C15A were prepared from DMAc and THF also, respectively.

But in the case of TPU/C25A, no peaks are observed in the XRD result of melt-mixed nanocomposites, while some peaks are noted in the solution mixed ones regardless of the solvent. This seems to be the manifestation that the shear force in melt-mixing facilitates the dispersion of C25A clays even without notable affinity between TPU and C25A, while XRD peaks observed in the solution mixed samples indicate the rather poor dispersion of C25A resulting from no significant affinity between TPU and C25A, which cannot be overcome by the weak shear force in solution mixing. Though C25A is

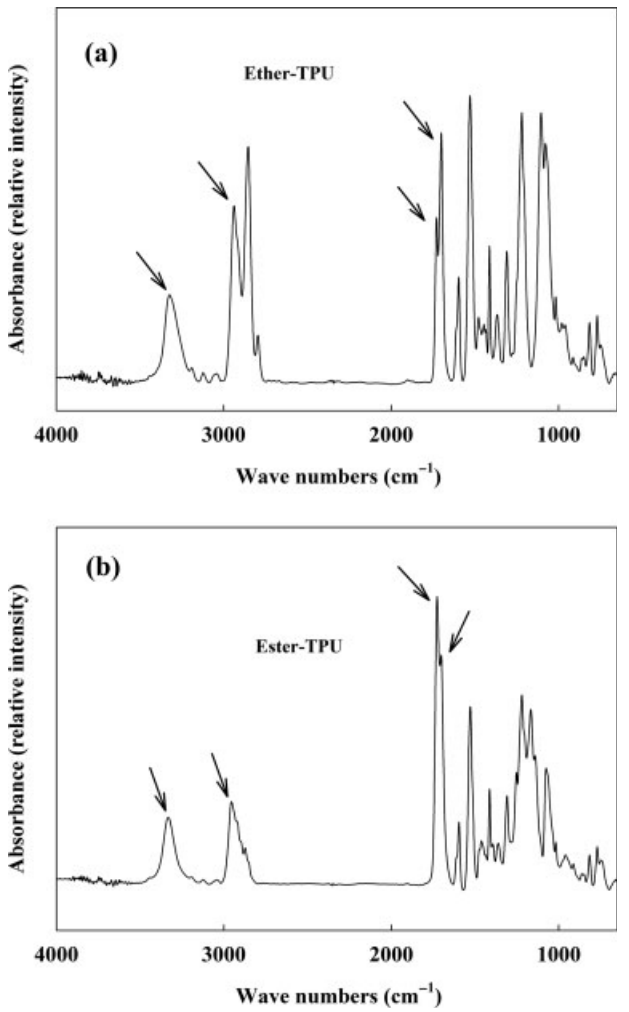

Figure 10 FTIR spectra (a) of ether-TPU and (b) of ester-TPU.

somewhat predispersed in THF, this does not give similar clay dispersion as in melt-mixed nanocomposites, which means that the affinity between polymers and clays of interest is very important for clay dispersion in solution mixing.

The above results exhibit that melt-mixing can give the good clay dispersion in the nanocomposites similar to that obtained by solution mixing with good solvents and even better clay dispersion in some cases, if the shear is high enough.

FTIR analysis

Ether-TPU nanocomposites

FTIR spectra of ether-TPU and ester-TPU are shown in Figure 10(a,b), respectively. In Figure 10(a), the —NH absorption peak of ether-TPU is observed at 3325 cm^{-1} which is due to the hydrogen bonded —NH in the urethane linkage, while carbonyl —C=O stretchings are shown at 1730 and 1701 cm^{-1} which are considered to be free and hydrogen bonded carbonyls, respectively. The —NH peak of ester-TPU is located at 3332 cm^{-1} and —C=O peaks are at 1728 and 1703 cm^{-1} as shown in Figure 10(b).

Typically the —NH groups in the urethane linkage form hydrogen bonds with carbonyls of the urethane linkage in the hard segment in both cases of ether-TPU and ester-TPU. The —NH groups are also able to form hydrogen bond with ether oxygen of ether-polyol in case of ether-TPU and with carbonyl of ester-polyol in case of ester-TPU. Therefore, careful examination of —NH and carbonyl peaks in the FTIR spectra can give some information on the morphology of the hard and soft segments in the polyurethane as done by Pattanayak and Jana.[30–32] In this regard, the ratio of area under the peaks of —NH (A_{NH}) and that of —CH (2860–2940 cm^{-1}) (A_{CH}) was calculated and shown in Table I. The area under —CH stretching was used as the internal standard. Also included in Table I is the ratio of areas under hydrogen-bonded carbonyl peaks (A_{HCO}) and free carbonyl peaks (A_{FCO}) for ether-TPU nanocomposites. The ratios in the Table I are average values from five measurements, and the range of deviation of measured values from the average values is ±0.01 for all cases except for A_{NH}/A_{CH} of ester-TPU/C15A prepared from DMAc solution where the deviation is ±0.03.

In the nanocomposites of ether-TPU/PM prepared from DMAc, the ratio of A_{NH}/A_{CH} (0.30) is observed to be the same as that of neat ether-TPU (0.31) as shown in Table I, while the ratio of A_{HCO}/A_{FCO} for ether-TPU/PM decreased to 2.64 from 2.70 of neat ether-TPU. Though clay PM was not well dispersed in TPU matrix but the decrease in the ratio of A_{HCO}/A_{FCO} indicates that clay PM is involved in the morphology change in ether-TPU/PM. Small decrease in 2θ values observed in the XRD results for ether- and ester-TPU/PM nanocomposites, as shown

TABLE I
Ratio of the Areas Under the Specific Peaks

		Ether-TPU		Ester-TPU
		A_{NH}/A_{CH}	A_{HCO}/A_{FCO}	A_{NH}/A_{CH}
From DMAc solution	TPU	0.30	2.70	0.69
	PM 5%	0.30	2.64	0.72
	C30B 5%	0.30	2.63	0.73
	C25A 5%	0.29	2.57	0.68
	C15A 5%	0.25	2.50	0.63
From THF solution	TPU	0.31	2.71	0.69
	PM 5%	0.31	2.71	0.76
	C30B 5%	0.30	2.70	0.73
	C25A 5%	0.30	2.73	0.68
	C15A 5%	0.29	2.68	0.64

A_{NH}: area under the hydrogen-bonded —NH peak); A_{CH}: area under the —CH stretching peak); A_{HCO}: area under the hydrogen-bonded —C=O peak); A_{FCO}: area under the free —C=O peak.

in Figure 1(a,b), can be interpreted in the same context. Clay PM may interfere the ordering of hard segments leading to decreasing the inter-urethane bonding between —NH and carbonyl resulting in the decrease in A_{HCO}/A_{FCO} ratio.

For ether-TPU/C30B or C25A nanocomposites prepared from DMAc solution, the ratio of A_{NH}/A_{CH} remains again the same as that (0.30) of neat ether-TPU, while values of the A_{HCO}/A_{FCO} of these nanocomposites decrease from that (2.70) of neat ether-TPU as shown in Table I. Decrease in this ratio of C30B nanocomposites indicates that hydrogen bonding between —NH and carbonyls in the urethane segments is reduced. Possibility is that the hydroxyl groups (—OH) in the modifier of C30B may form hydrogen bonding with carbonyl groups in hard segment resulting in decrease in the inter-urethane hydrogen bonding. Some of the hydroxyls in the C30B modifier may still form hydrogen bonding with ether oxygen in the soft segment. As observed in TEM analysis, well-dispersed clay layers of C30B in TPU matrix support this scenario in view of the observation that clay C30B is very well distributed throughout the matrix, which appears to cover both the urethane hard segment and the soft segment polyol phase. In the ether-TPU/C25A or 15A nanocomposites, the ratios of A_{HCO}/A_{FCO} (2.57 or 2.50) also decrease as compared with the neat ether-TPU. Since there is no functional group that can form specific interaction with urethane hard segments in these clays, C25A or 15A may be incorporated into the soft segments rather than hard segments. Then the decrease in A_{NH}/A_{CH} and A_{HCO}/A_{FCO} may be attributed not to the interaction of clay with hard segments, but rather to the reduced hard segment inter-urethane hydrogen bonding from decrease in hard segment ordering as well as the reduced hydrogen bonding between —NH of hard segment and ether oxygen in soft segment, which were caused by the addition of clay C25A or C15A.

The value of the above ratios for ether-TPU/clay prepared from THF solution is also shown in Table I. The ratios of A_{NH}/A_{CH} show the similar values to the ones from DMAc solutions. The difference in A_{HCO}/A_{FCO} values from those obtained from DMAc is that the ratios of samples from THF are generally higher than those of the ones from DMAc, but the trend is still similar.

Notable differences in A_{HCO}/A_{FCO} ratios are observed for the case of C25A and C15A nanocomposites, where much higher values were observed for the A_{HCO}/A_{FCO} ratio in nanocomposites prepared from THF as compared with the ones from DMAc. Outcomes of C15A nanocomposites may be interpreted as the result of good dispersion of C15A in THF when compared with that in DMAc as shown in Figure 9. Well dispersed clay C15A may induce the phase separation between hard and soft segments of TPU resulting in more ordering in hard segments. This leads to the higher interurethane hydrogen bonding and the lower hydrogen bonding between —NH and ether oxygen, which gave the observed ratios of A_{NH}/A_{CH} and A_{HCO}/A_{FCO}. The result for ether-TPU/C25A may be interpreted in the similar context but still the highest value of A_{HCO}/A_{FCO} for ether-TPU/C25A nanocomposites cannot be explained solely by the state of good clay dispersion in THF, since C25A showed slightly better dispersion in DMAc as shown in Figure 9. In this regard, the property of the solvent itself as well as the dispersion state of clay in the solvent may be thought to contribute to the formation of the final morphology of TPU nanocomposites.

Ester-TPU nanocomposites

In ester-TPU/PM nanocomposites prepared from DMAc solution, the ratio of A_{NH}/A_{CH} shown in Table I increases to 0.72 from 0.69 of neat ester-TPU indicating that more hydrogen bonding involving —NH formed. Clay PM is thought to promote phase separation between hard segments and soft segments resulting in more ordering in the hard segments and more interurethane hydrogen bonding. Therefore —NH groups may form hydrogen bonding mostly with carbonyls in the hard segments resulting in the higher value of A_{NH}/A_{CH}. In ester-TPU/C30B nanocomposites, even higher value (0.73) of A_{NH}/A_{CH} was observed when compared with that (0.72) of PM nanocomposites. But in this case, the reason for increase in this ratio may be different from PM nanocomposites. Clay layers of C30B well dispersed in ester-TPU matrix may include more hydrogen bonding involving —NH groups. In the ester-TPU/C25A nanocomposites, the ratio of A_{NH}/A_{CH} slightly decreased to 0.68 from 0.69 of neat ester-TPU. This decrease in ratio suggests that hydrogen bonding between —NH and carbonyls in the hard segment or in ester polyol decreased by the addition of clay C25A. More decrease in the ratio of A_{NH}/A_{CH} (0.61) for ester-TPU/C15A nanocomposites prepared from DMAc solution as compared with ester-TPU/C25A may be explained in the same context.

When ester-TPU/clay nanocomposites were prepared in THF, similar trends and even similar values as the case in DMAc were observed. This may partly arise from the fact that the hydrogen bonding in ester-TPU nanocomposites formed between —NH and the carbonyls of soft segment polyols as well as those of hard segments, where the effect of solvent on the morphology becomes less than the ether-TPU cases.

Dynamic mechanical properties

The reinforcing effect of clay in the nanocomposites was investigated by means of dynamic mechanical

analysis. Figure 11(a,b) present the storage modulus (E') of the ether-TPU nanocomposites containing 5 wt % different clay types prepared in DMAc and THF, respectively, as a function of temperature. In the Figure 11(a,b), it can be seen that the higher storage moduli of the ether-TPU/clay nanocomposites were shown than that of the neat ether-TPU. It is believed that the restricted movement of polymer chain by dispersed clay layers resulted in the increase in storage modulus.

The nanocomposites incorporating C30B displayed a higher value of the storage modulus when compared with the other clays over most of the temperature ranges being examined regardless of solvent types. This again indicates that the interaction between clays and polymers is more important in determining the properties of nanocomposites than the predispersion state of clay in the solvent during preparation. But still the state of clay predispersion as well as the effect of the solvent on the final morphology becomes important when there is no specific interaction such as in PM, C25A, or C15A cases, since difference in storage moduli are observed in these nanocomposites. C25A nanocomposites show a fairly good storage modulus followed by C15A and PM nanocomposites which exhibit similar values. Figure 12(a,b) shows the storage moduli of ester-TPU nanocomposites prepared in DMAc and THF, respectively. Similar trends with ether-TPU nanocomposites were observed. From the above results, it can be inferred that the clay dispersion state in the nanocomposites plays some role in determining the storage modulus when there is no interaction between clays and polymer or even the interaction between the two is rather weak.

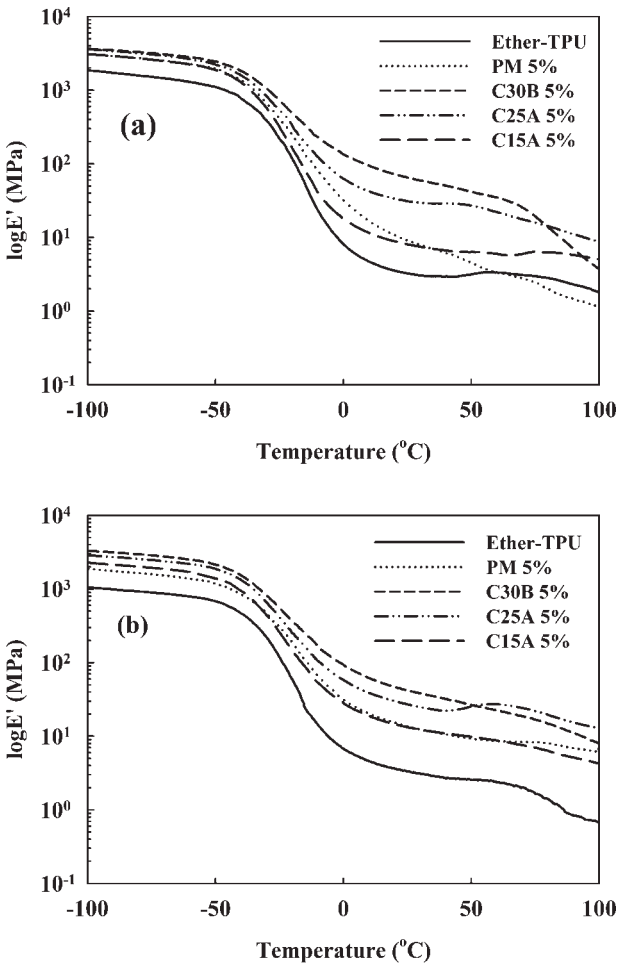

Figure 11 The storage modulus (log E') for ether-TPU nanocomposites containing 5 wt % clay for different clay types prepared in (a) DMAc and (b) THF.

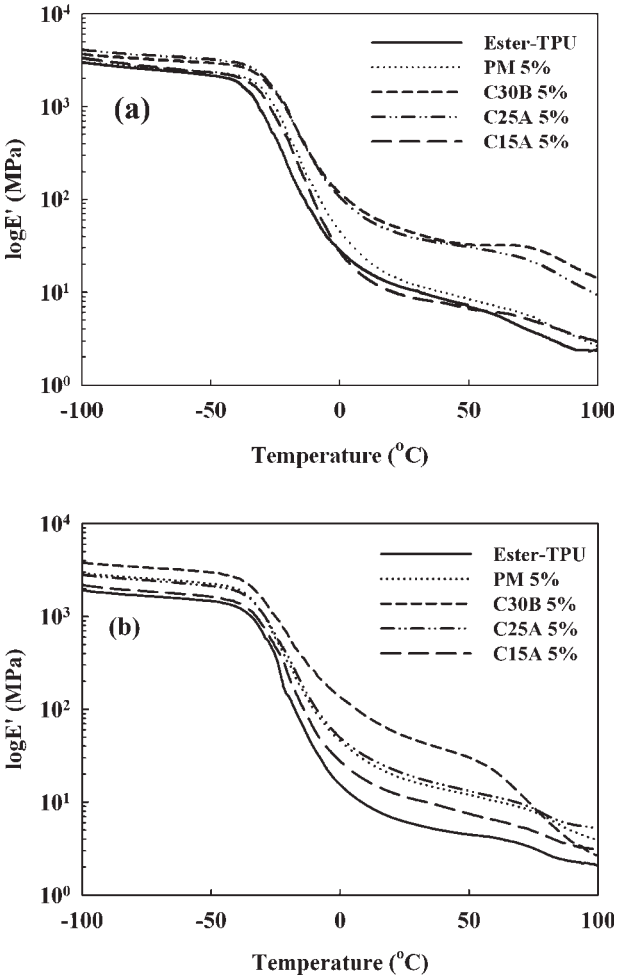

Figure 12 The storage modulus (log E') for ester-TPU nanocomposites containing 5 wt % clay for different clay types prepared in (a) DMAc and (b) THF.

CONCLUSIONS

Ether-based and ester-based TPU/clay nanocomposites were prepared via solution mixing method using two different solvents, DMAc and THF. From XRD and TEM results, very good dispersion of clay

C30B were observed for both ether- and ester-based TPU nanocomposites. The ether and ester-TPU nanocomposites containing C25A and C15A showed the different state of dispersions when they were prepared by two different solvents. Better dispersion of clay C30B was observed in DMAc dispersion, while THF gave the better result to C15A. This is thought to be due to the difference in solubility parameter differences between the solvents and the clays. Although this result suggests that the interaction between clays and solvents plays some role in the dispersion of clay in TPU nanocomposites, this becomes meaningful when there is no specific interaction between the clay and polymers or the interaction between the two is rather weak. The compatibility between clays and polymers becomes dominating in determining the final properties of nanocomposites, if there exists a specific interaction between the two such as in the case of nanocomposites containing C30B where good dispersion of clays was observed in this case regardless of the solvent.

Clay dispersion and the morphology of the nanocomposites prepared from DMAc and THF were analyzed using the ratio of free and hydrogen-bonded carbonyls as well as the hydrogen-bonded —NH peak areas in FTIR analysis. Morphologies of the nanocomposites were thought to be determined not only by the state of clay dispersion in different solvents but also by the effect of the solvent on the phase behavior of matrix polymers. Storage modulus measurements also supported this argument.

This study was supported by the Center for Environmental and Clean Technologies designated by MOCIE in The University of Suwon. The authors acknowledge the efforts of the Korea Basic Science Institute for taking nice TEM pictures.

References

1. Giannelis, E. P. Adv Mater 1996, 8, 29.
2. Giannelis, E. P.; Krishnamoorti, R.; Manias, E. Adv Polym Sci 1999, 138, 107.
3. LeBaron, P. C.; Wang, Z.; Pinnavaia, T. J. Appl Clay Sci 1999, 15, 11.
4. Vaia, R. A.; Price, G.; Ruth, P. N.; Nguyen, H. T.; Lichtenhan, J. Appl Clay Sci 1999, 15, 67.
5. Biswas, M.; Sinha Ray, S. Adv Polym Sci 2001, 155, 167.
6. Giannelis, E. P. Appl Organomet Chem 1998, 12, 675.
7. Xu, R.; Manias, E.; Snyder, A. J.; Runt, J. Macromolecules 2001, 34, 337.
8. Bharadwaj, R. K. Macromolecules 2001, 34, 1989.
9. Messersmith, P. B.; Giannelis, E. P. J Polym Sci Part A: Polym Chem 1995, 33, 1047.
10. Yano, K.; Usuki, A.; Okada, A.; Kurauchi, T.; Kamigito, O. J Polym Sci Part A: Polym Chem 1993, 31, 2493.
11. Kojima, Y.; Usuki, A.; Kawasumi, M.; Fukushima, Y.; Okada, A.; Kurauchi, T.; Kamigaito, O. J Mater Res 1993, 8, 1179.
12. Gilman, J. W.; Kashiwagi, T.; Lichtenhan, J. D. SAMPE J 1997, 33, 40.
13. Gilman, J. W. Appl Clay Sci 1999, 15, 31.
14. Bourbigot, S.; LeBras, M.; Dabrowski, F.; Gilman, J. W.; Kashiwagi, T. Fire Mater 2000, 24, 201.
15. Gilman, J. W.; Jackson, C. L.; Morgan, A. B.; Harris, R., Jr.; Manias, E.; Giannelis, E. P.; Wuthenow, M.; Hilton, D.; Phillips, S. H. Chem Mater 2000, 12, 1866.
16. Sinha Ray, S.; Yamada, K.; Okamoto, M.; Ueda, K. Nano Lett 2002, 2, 1093.
17. Wang, D.; Zhu, J.; Yao, Q.; Wilkie, C. A. Chem Mater 2002, 14, 3837.
18. Vaia, R. A.; Giannelis, E. P. Macromolecules 1997, 30, 9189.
19. Sinha Ray, S.; Okamoto, M. Prog Polym Sci 2003, 28, 1539.
20. Theng, B. K. G. Formation and Properties of Clay-Polymer Complexes; Elservier: Amsterdam, 1979.
21. Yu, X.; Nagarajan, M. R.; Grasel, T. G.; Gibson, P. E.; Cooper, S. L. J Polym Sci Part B: Polym Phys 1985, 23, 2319.
22. Hwang, K. K. S.; Yang, C.; Cooper, S. L. Polym Eng Sci 1981, 21, 1027.
23. Chen, W. Int Polym News 1991, 4, 1.
24. Van Bogart, J.; Gibson, P. E.; Cooper, S. L. J Polym Sci Part B: Polym Phys 1983, 21, 65.
25. Harris, R. F.; Joseph, M. D.; Davidson, C.; De Porter, C. D.; Dais, V. A. Polym Prepr 1989, 30, 235.
26. Li, Y.; Gao, T.; Liu, J.; Linliu, K.; Desper, C. R.; Chu, B. Macromolecules 1992, 25, 7365.
27. Wang, Z.; Pinnavaia, T. J. Chem Mater 1998, 10, 3769.
28. Tien, Y. I.; Wei, K. H. Macromolecules 2001, 34, 9045.
29. Tien, Y. I.; Wei, K. H. Polymer 2001, 42, 3213.
30. Pattanayak, A.; Jana, S. C. Polymer 2005, 46, 3275.
31. Pattanayak, A.; Jana, S. C. Polymer 2005, 46, 3394.
32. Pattanayak, A.; Jana, S. C. Polymer 2005, 46, 5183.
33. Dan, C. H.; Lee, M. H.; Kim, Y. D.; Min, B. H.; Kim, J. H. Polymer 2006, 47, 6718.
34. Jang, B. N.; Wang, D.; Wilkie, C. A. Macromolecules 2005, 38, 6533.